

Supporting Information

Seeger-Nukpezah et al. 10.1073/pnas.1301904110

SI Materials and Methods

Drug Treatment. STA-2842 was formulated in 5% dextrose titrated to pH 4 and was administered by tail vein injection in anesthetized mice under sterile conditions using a volume of 10 μ L/g body weight. Vehicle-treated mice were injected with 5% dextrose, pH 4. To investigate the activity of STA-2842 on early kidney disease, mice were treated with STA-2842 for 5 mo, starting 2–3 d after *Pkd1* deletion of the gene for polycystic kidney disease, *Pkd1*. In a first cohort, treatment began with a weekly schedule up to 4 mo of age, including 1 wk off in the third month of age, followed by a biweekly schedule from 4–6 mo of age. Blood samples were collected 24 h after the 16th injection, and the mice were euthanized to collect kidneys for histopathological and biochemical analysis. In a second cohort, mice were dosed weekly with STA-2842 for 10 wk starting at 4 mo of age. Blood samples were collected 24 h after the 11th dose (10 wk of treatment), and the mice were euthanized to collect kidneys for histopathological and biochemical analysis. For the analysis of kidney and plasma concentration of STA-2842, female mice were dosed once with 75 mg/kg STA-2842, and kidneys and blood samples were collected either 12 or 48 h later.

Tissue Preparation, Histology, and Immunohistochemical Detection. Tissues were collected and fixed in 10% phosphate-buffered formaldehyde (formalin) for 24–48 h, dehydrated, and embedded in paraffin. H&E-stained sections were used for morphological evaluation, and unstained sections were used for immunohistochemical studies. Immunohistochemical staining was performed on 5- μ m formalin-fixed paraffin-embedded sections. After deparaffinization and rehydration, sections were subjected to heat-induced epitope retrieval by steaming in 0.01 M citrate buffer (pH 6.0) or EDTA (pH 9.0) for 20 min. After endogenous peroxidase activity was quenched with 3% hydrogen peroxide for 20–30 min and nonspecific protein binding was blocked with goat serum, sections were incubated overnight with primary monoclonal antibodies to Ki67 (Rat anti-mouse, 1:100; DAKO) and cleaved caspase 3 (Cell Signaling) at 4 °C, followed by biotinylated goat anti-Rat IgG (1:200; DAKO) for 30 min. The antibody complexes were detected with the labeled streptavidin-biotin system (DAKO) and were visualized with the chromogen 3,3'-diaminobenzidine. Primary antibody was replaced with nonspecific rabbit IgG as a negative control. To minimize the endogenous biotin background, immunodetection for anti-phospho-Erk1/2 (pThr202/pTyr204) (rabbit, 1:400; #4370, Cell Signaling) and anti-Hsp90 α (rabbit, 1:800; #NB120-2928, Novus Biologicals) was performed with the Dako Envision+ polymer system.

Western Blotting and Antibodies. To analyze the expression levels of individual proteins, cells were lysed and resolved by SDS-PAGE. Western blotting was performed using standard procedures and was developed by chemiluminescence using Super Signal West Pico and Femto substrate (Thermo Fisher Scientific). Primary antibodies included anti-signal transducer and activator of transcription 3 (STAT3) (#9139; Cell Signaling), anti-phospho-STAT3 (#9139; Cell Signaling), anti-heat shock protein 70 (HSP70) (#ADI-SPA-820; Enzo), anti-heat shock protein 90 (HSP90) (#ADI-SPA-835; Enzo), anti-phospho-ERK Thr202/204 (#9101; Cell Signaling), anti-ERK (#4696; Cell Signaling), anti-phospho-AKT^{S473} (#4060; Cell Signaling), anti-AKT (#9272; Cell Signaling), anti-S6 (#2317; Cell Signaling), anti-phospho-S6^{S235/236} (#4858; Cell Signaling), anti-heat shock protein 27

(Hsp27) (ADI-SPA-830; Enzo), anti-EGF receptor (EGFR) (#2646; Cell Signaling), anti-phospho-EGFR^{Y1068} (#3777; Cell Signaling), anti-GAPDH (Millipore), and mouse anti- β -actin conjugated to HRP (#ab49900; Abcam). Secondary anti-mouse and anti-rabbit antibodies (GE Healthcare) were used at a dilution of 1:10,000, and anti-rat HRP-conjugated antibodies (Cell Signaling) were used at a dilution of 1:2,000. Quantification of signals on Western blots was done using National Institutes of Health (NIH) ImageJ Imaging and Processing Analysis Software with signaling intensity normalized to β -actin or GAPDH.

MRI Performance and Image Analysis. Mice were imaged in a vertical bore MR system at a field strength of 7 T, using a Bruker DRX300 spectrometer, ParaVision 3.0.2 software (Bruker), and a single tuned ¹H cylindrical radiofrequency coil. Following acquisition of a low-resolution scout scan in the axial plane, a coronal scan was set to cover the entire volume of both kidneys. A rapid acquisition of refocused echoes (RARE) pulse sequence was used, because it previously has been shown in RARE sequences in preclinical models of polycystic kidney disease that cysts exhibit high intensity in the MR images and are easily distinguishable from the surrounding tissues (1–3). The acquisition parameters for the RARE scan were echo time = 17.6 ms, rare factor = 8, effective echo time = 73.6 ms, repetition time = 4,500 ms, averages = 4, slice thickness = 0.75 mm, field of view = 2.56 mm, in-plane resolution = 0.1 mm, number of slices = 28. The total acquisition time was 10 min, 3 s, which was well tolerated by the mice. During the imaging procedure mice were anesthetized with 1–2% isoflurane in O₂. Images show the size and texture of the complete kidneys.

Kidney and cyst volume were quantified using NIH ImageJ, an open-source image analysis program. Kidney volume was estimated as previously described (4) by manually surrounding kidney parenchyma excluding the renal pelvis and summing up the products of area measurements of contiguous images and slice thickness. A semiautomatic threshold approach was used to estimate cyst volume (5, 6). Subsequently isolated kidney areas were prepared using defined settings for background subtraction (rolling ball radius: 20 pixels) and band passing (fast Fourier transform band pass filter with structures 3–40 pixels). The threshold was set for each kidney based on the original images by targeting threshold values designating the transition between parenchyma and cyst that could be detected at the border of larger cysts in the kidneys.

Pharmacokinetic analysis. Plasma. Three hundred microliters of acetonitrile containing the internal standard (a derivative of STA-12-2842) were added to 50 μ L of plasma samples, mixtures were centrifuged to remove insoluble debris, and the result supernatants were dried under nitrogen and then were reconstituted with 200 μ L of 25:75 (vol/vol) acetonitrile:water for analysis by LC-MS/MS.

Tissue. Liver and kidney samples were homogenized in three volumes of PBS with a probe homogenizer. Three hundred microliters of acetonitrile containing the internal standard (a derivative of STA-12-2842) were added into 50 μ L of tissue homogenate, and the mixtures were centrifuged at 4,506 \times g for 10 min at 4 °C. The resulting supernatants were dried under nitrogen and then were reconstituted with 200 μ L of 25:75 (vol/vol) acetonitrile:water for analysis by LC-MS/MS.

Plasma and tissue sample analysis. Plasma and tissue samples were analyzed with an Agilent 1100 HPLC interfaced to an API 4000

tandem mass spectrometer (Applied Biosystems) using a SymmetryShield RP18 column (5 μ m, 2.1 \times 100 mm; Waters) at a flow rate of 0.5 mL/min. The aqueous mobile phase consisted of 10 mM ammonium acetate, and the organic mobile phase consisted of 10 mM ammonium acetate in 90:10 (vol/vol) acetonitrile:water. Total run time was 5 min with the gradient elution. Detection was achieved with turbo ion spray ionization under the positive-ion mode by multiple reaction monitoring.

Statistical Analysis. For statistical analyses, we used generalized linear models assuming appropriate link and family functions. In particular, we assumed either Gaussian families with identity links or Gamma families with log links. The Gamma families allowed us to model nonnormally distributed data appropriately. For longitudinal models, we estimated the models by Generalized Estimating Equations (i.e., GEE, growth curve models) to account for correlation within a mouse's observations over time. We used appropriate working correlation matrices for the GEE estimated models (e.g., ref. 6). For figures, we used restricted cubic splines to model temporal trends visually (7). To account for multiple hypotheses testing, we used the false discovery rate (8) to assist with the identification of proteins of interest (e.g., Fig. 1C).

Network Construction. Protein–protein interactions for the genes for polycystic kidney disease, *PKD1* and *PKD2*, were retrieved

using the Ingenuity (www.ingenuity.com/index.html), String, and iRefScape metasearch engines. Genes associated with PKD were retrieved from Ingenuity, GeneCards (www.genecards.org/), National Center for Biotechnology Information (www.ncbi.nlm.nih.gov/sites/entrez?db=gene), HuGE Navigator (www.hugenavigator.net/HuGENavigator/home.do), Kyoto Encyclopedia of Genes and Genomes (www.genome.jp/kegg/disease/), The Genetic Association Database (<http://geneticassociationdb.nih.gov/>), The Human Gene Mutation Database (www.hgmd.cf.ac.uk/ac/index.php), and Comparative Toxicogenomics Database (<http://ctdbase.org/>). HSP90 interactors were retrieved using the Ingenuity (www.ingenuity.com/index.html) and String metasearch engines, as well as the Hsp90 interaction database (HSP90Int.db; www.picard.ch/Hsp90Int/index.php). Proteins in common in the HSP90 and PKD datasets were selected; interactions between these proteins were retrieved from the String database and visualized in Cytoscape (www.cytoscape.org). As quality control, genes nominated by only one source for HSP90 and PKD association were not included, and interactions were shown only for a subset of genes highly relevant to the disease. The *P* value for enrichment was calculated using hypergeometric distribution with the number of characterized human genes taken from the Ingenuity database (19,600).

1. Kobayashi H, et al. (2004) Micro-MRI methods to detect renal cysts in mice. *Kidney Int* 65(4):1511–1516.
2. Hadjidemetriou S, Reichardt W, Hennig J, Buechert M, von Elverfeldt D (2011) Volumetric analysis of MRI data monitoring the treatment of polycystic kidney disease in a mouse model. *MAGMA* 24(2):109–119.
3. Zhou X, et al. (2010) Polycystic kidney disease evaluation by magnetic resonance imaging in ischemia-reperfusion injured PKD1 knockout mouse model: Comparison of T2-weighted FSE and true-FISP. *Invest Radiol* 45(1):24–28.
4. Reichardt W, et al. (2009) Monitoring kidney and renal cyst volumes applying MR approaches on a rapamycin treated mouse model of ADPKD. *MAGMA* 22(3):143–149.
5. Lee YR, Lee KB (2006) Reliability of magnetic resonance imaging for measuring the volumetric indices in autosomal-dominant polycystic kidney disease: Correlation with hypertension and renal function. *Nephron Clin Pract* 103(4):c173–c180.
6. Shults J, Ratcliffe SJ, Leonard M (2007) Improved generalized estimating equation analysis via xtqls for implementation of quasi-least squares in STATA. *Stata J* 7(2):147–166.
7. Harrell FE (2001) *Regression Modeling Strategies* (Springer, New York), pp 20–24.
8. Benjamini Y, Hochberg Y (1995) Controlling the False Discovery Rate: A practical and powerful approach to multiple testing. *J R Stat Soc, B* 57(1):289–300.

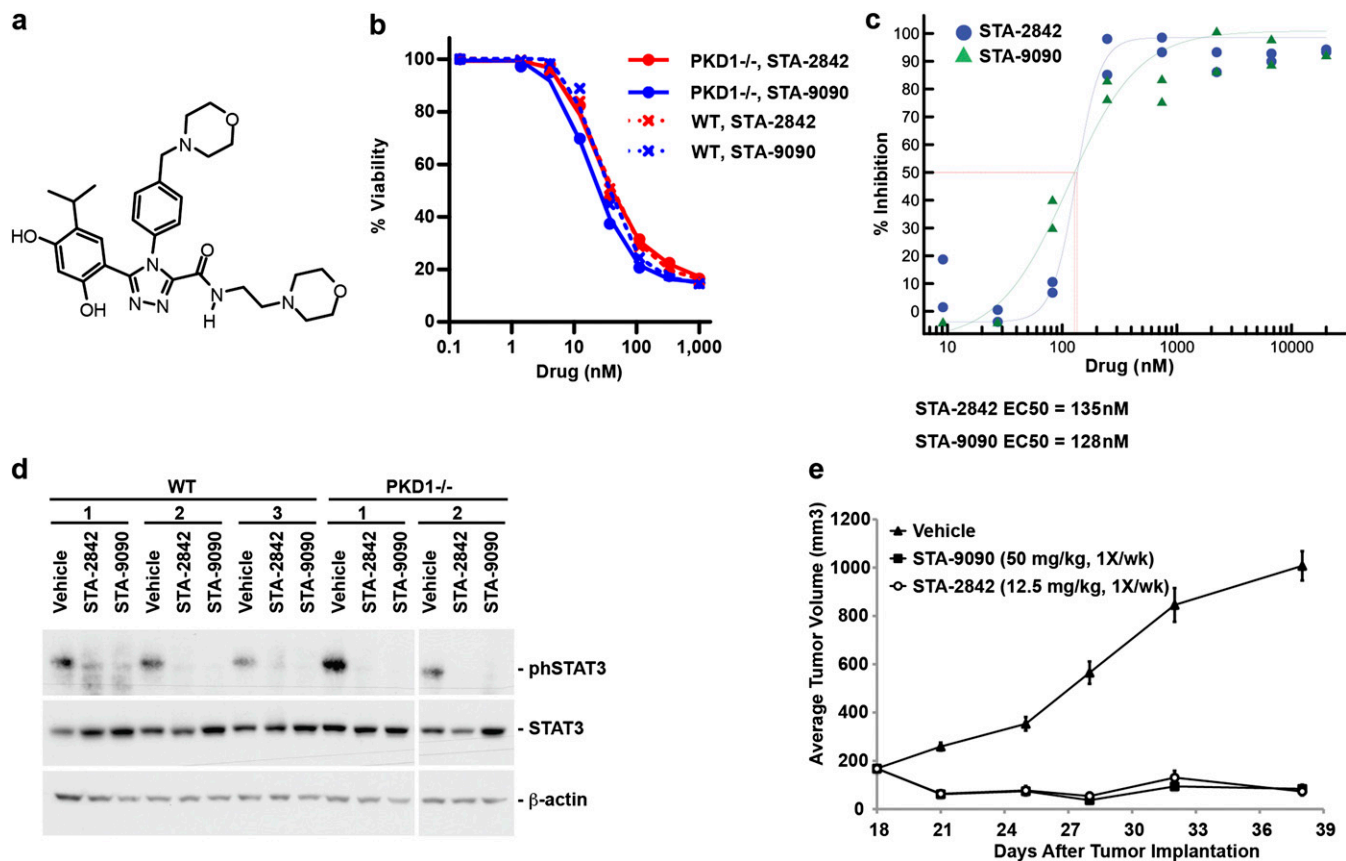


Fig. S1. (A) STA-2842 (molecular weight = 550.6) is a resorcinolic triazole compound that exhibits competitive binding for the N-terminal ATP pocket of HSP90. STA-2842 forms a salt with specific acids resulting in a water-soluble powder. (B) Multiple independent preparations of primary kidney cells derived from *Pkd1*^{-/-} and WT mice and used at early passage (fewer than eight passages) were used to assess cell viability 72 h after treatment with STA-2842 (red) or STA-9090 (blue). (C) Comparison of STA-2842 with STA-9090 regarding the inhibition of HSP90- α , as determined by fluorescent polarization was performed as described previously (1). (D) Western blot analysis of the indicated proteins after treatment with 250 nM STA-2842, STA-9090, or vehicle in multiple independent preparations of primary kidney cells from *Pkd1*^{-/-} and control mice. (E) Efficacy study comparing STA-2842 and STA-9090 in MV4-11:00 acute myeloid leukemia (AML) xenografts. Female CB.17 (SCID) mice (Charles River Laboratories) at 8 wk were inoculated s.c. with MV4-11:00 AML cells (5E6). Mice bearing established tumors (~200 mm³) were randomized into treatment groups of three mice and were dosed i.v. with vehicle, STA-9090, or STA-2842 once weekly for 3 wk. Tumor volumes (V) were calculated by caliper measurements of the width (W), length (L), and thickness (T) of each tumor using the formula: $V = 0.5236(LWT)$.

1. Jin L, et al. (2011) Antiproliferative and proapoptotic activity of GUT-70 mediated through potent inhibition of Hsp90 in mantle cell lymphoma. *Br J Cancer* 104(1):91–100.

STA-2842
 115 Assays Tested
 3 Interactions Mapped
 S-Score(35) = 0,03

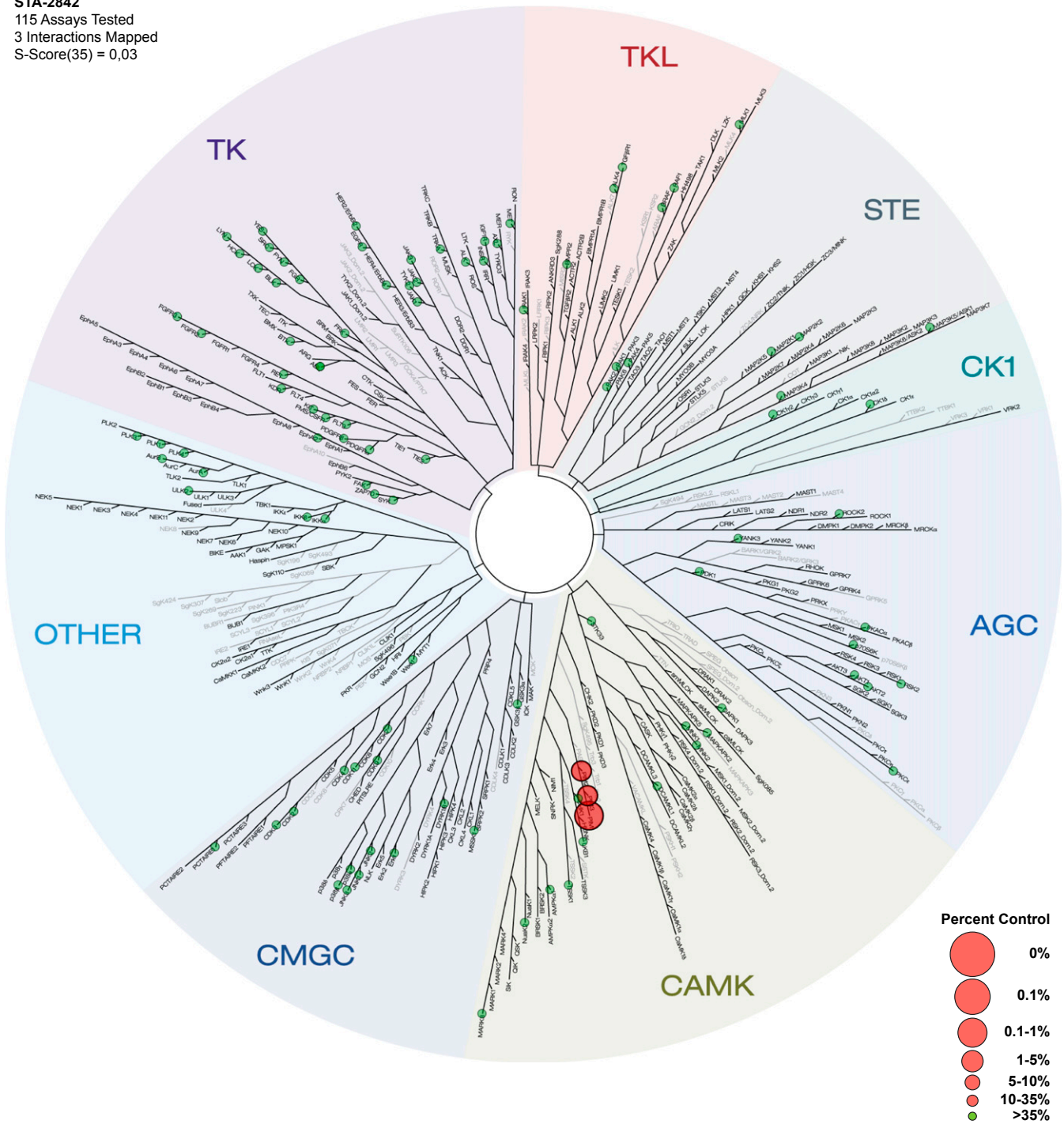


Fig. S2. DiscoverX KINOMEScan (DiscoverX) was performed for STA-2842 (10 μ M) against 97 distinct kinase targets using methods previously described (1). The three kinases found to bind at this high concentration [proviral integration site for Moloney murine leukemia virus (PIM) kinases 1,2,3] are marked with red circles; larger circles indicate higher-affinity binding. Green dots represent weaker compound/kinase interactions with a percent control value ≤ 35 . The image was generated using TREEspot Software Tool and is reprinted with permission from KINOMEScan, a division of DiscoverX Corporation, © DISCOVERX CORPORATION 2010. AGC, protein kinase A, G, and C families; CAMK, Ca²⁺/calmodulin-dependent kinase; CK1, casein kinase 1 family; CMGC, kinase group CMGC; STE, kinase group STE; TK, tyrosine kinase group; TKL, tyrosine kinase-like kinases.

1. Davis MI, et al. (2011) Comprehensive analysis of kinase inhibitor selectivity. *Nat Biotechnol* 29(11):1046–1051.

STA-2842
 115 Assays Tested
 3 Interactions Mapped
 S-Score(35) = 0,03

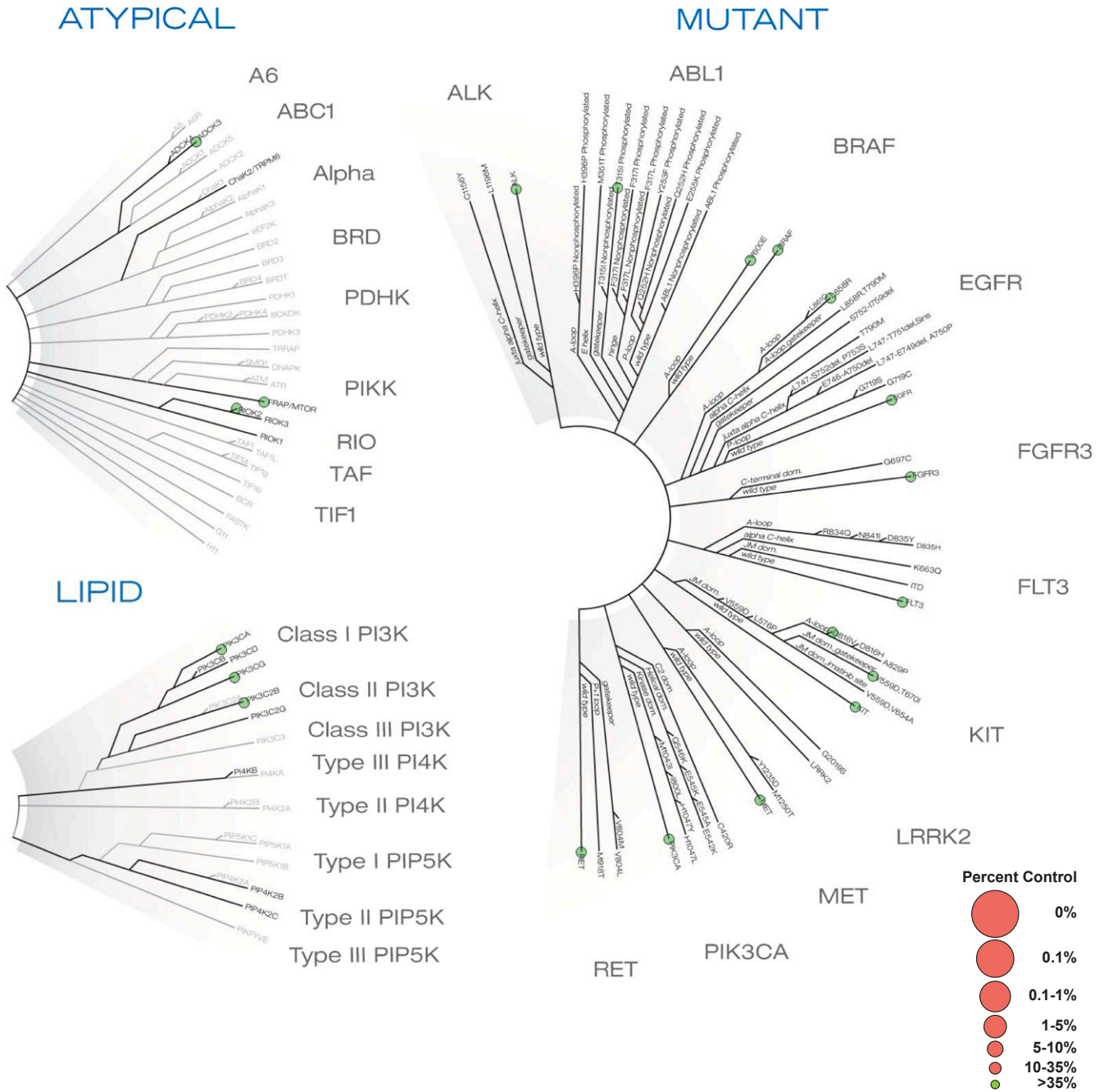


Fig. S3. Expansion of DiscoveRx KINOMEScan, including clinically relevant mutant, lipid, and atypical kinases.

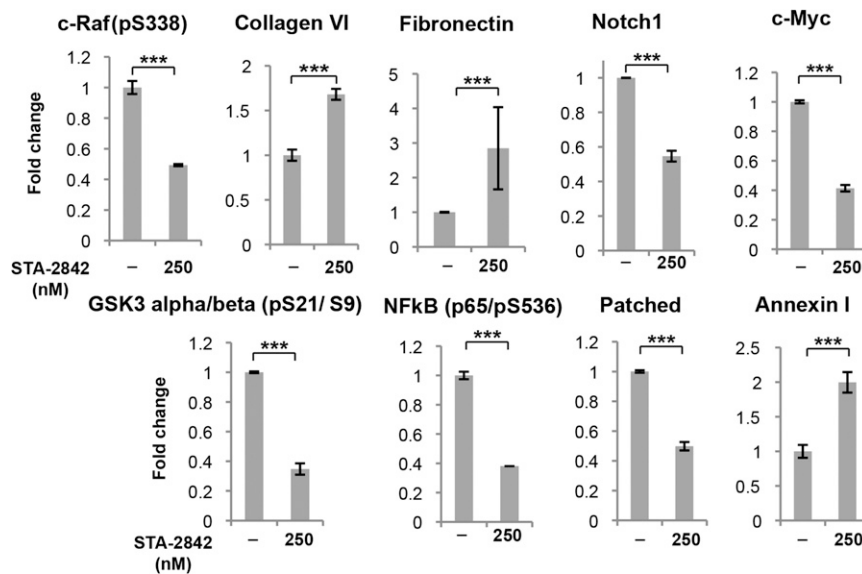


Fig. S4. Quantification of selected targets of STA-2842 inhibition detected by reverse phase protein array (RPPA) analysis. Graph represents specific targets of inhibition by STA-2842, selected from RPPA analysis of two independent, early-passage isolates of *Pkd1*^{-/-} kidney cells following treatment with 250 nM STA-2842 versus vehicle for 24 h. *** $P \leq 0.001$. Data are expressed as mean \pm SEM. c-Myc, Myc proto-oncogene protein; c-Raf, RAF proto-oncogene serine/threonine-protein kinase; GSK3, glycogen synthase kinase 3.

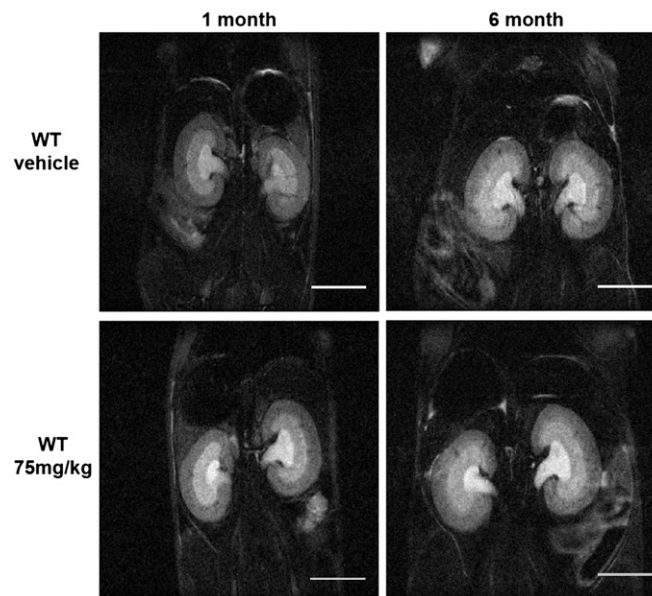


Fig. S5. MRI images of kidneys of STA-2842-treated versus WT mice. MRI images of drug- or vehicle-treated WT mice of the "Early cohort" (treatment began with a weekly schedule up to 4 months of age, including 1 wk off in the third month of age, followed by a biweekly schedule from 4–6 months of age) at the indicated time points. (Scale bar, 0.5 cm.)

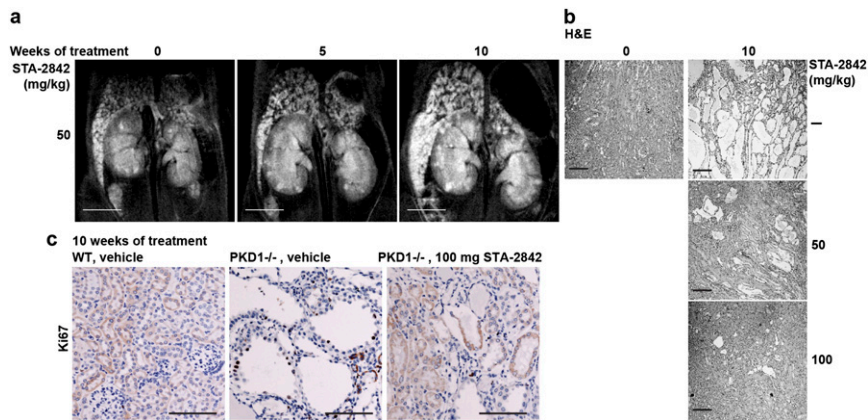


Fig. S6. Additional MRI images and immunohistochemical analysis of kidney sections. (A) Representative MRI images of *Pkd1*^{-/-} mice treated with 50 mg/kg STA-2842 at the indicated time points (also see Fig. 3B). (Scale bar, 0.5 cm.) (B) H&E-stained kidney sections of *Pkd1*^{-/-} mice corresponding to Fig. 3B, with an additional section from 4-mo-old mice taken at the beginning of treatment. (Scale bar, 200 μm.) (C) Representative images of Ki67⁺ stained kidney sections of 6-mo-old *Pkd1*^{-/-} and WT mice treated with vehicle or 100 mg/kg STA-2842 for 10 wk. For quantification see Fig. 3H. (Scale bar, 100 μm.)

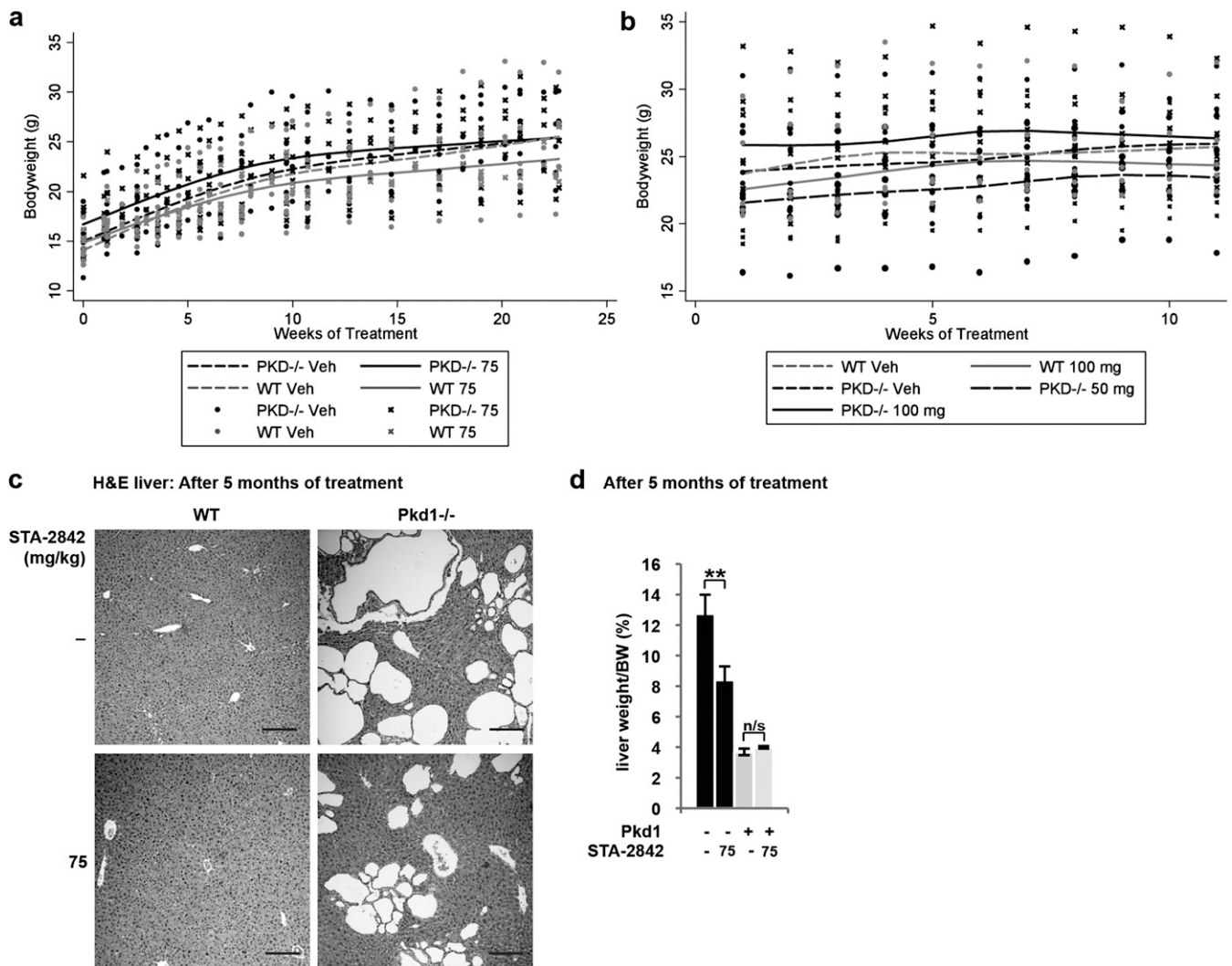


Fig. S7. Weight curve of *Pkd1*^{-/-} and control mice. (A and B) Weight curves showing body weight (in grams) of *Pkd1*^{-/-} and control mice over the full term of treatment for the cohorts of mice receiving early (A) and late (B) treatment. There was no significant difference between drug- and vehicle-treated mice in the WT or the *Pkd1*^{-/-} group over time (corrected for baseline weight). (C) Representative images of H&E-stained liver sections of WT or *Pkd1*^{-/-} mice treated with vehicle or 75 mg/kg STA-2842 for 5 mo. (D) Effect of STA-2842 on ratio of liver to body weight (BW); $n = 6$ for each WT group and $n = 16$ for each *Pkd1*^{-/-} group. $**P = 0.003$.

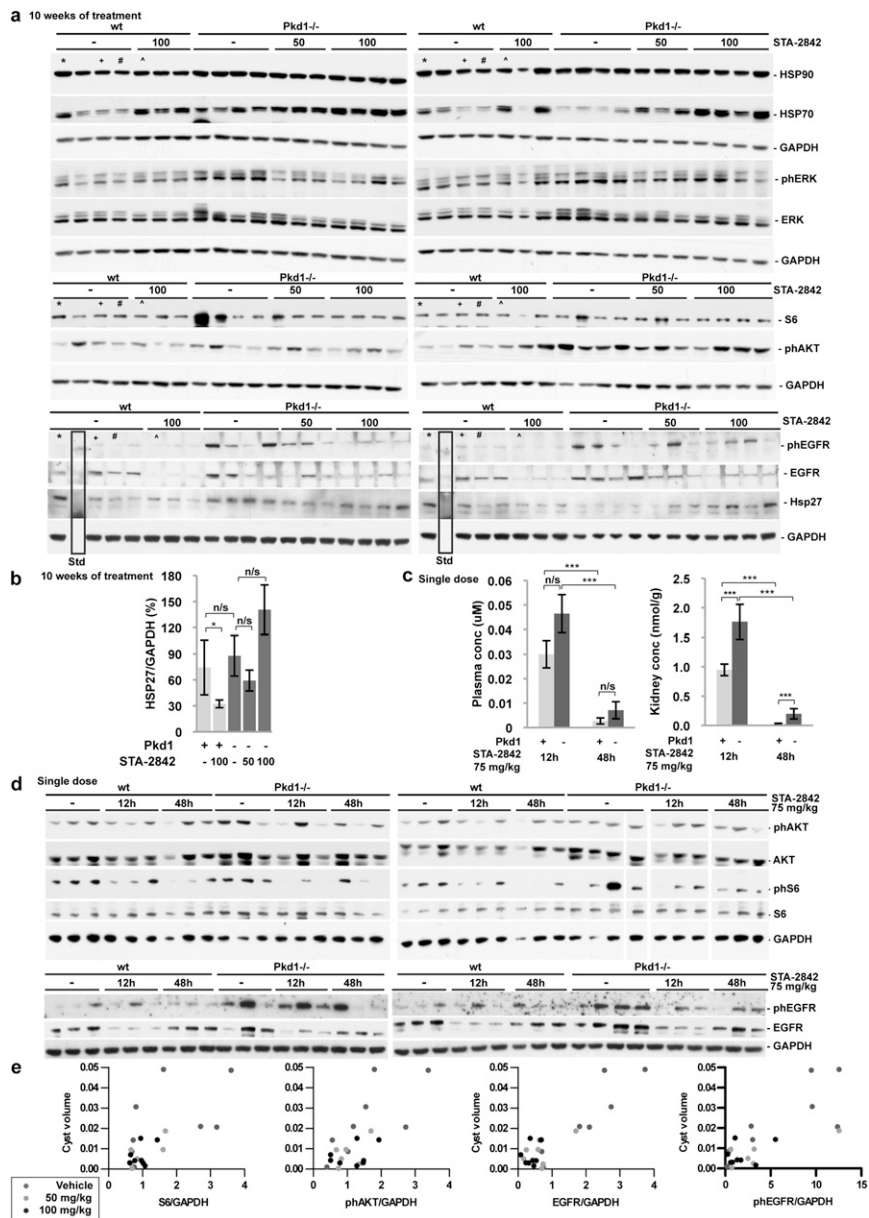


Fig. S8. Western blot analysis of *Pkd1*^{-/-} and control mice. (A) Western Blot analysis of kidney lysates of 6-mo-old *Pkd1*^{-/-} or control mice treated from 4 mo of age for 10 wk with 50 mg/kg or 100 mg/kg STA-2842 or vehicle, analyzed with indicated antibodies. Each lane shown represents lysates from an independent animal, except that lysates marked *, +, #, and ^ are loaded as internal references on both membranes to ensure normalization of signal. Std, standard. (B) Results for Hsp27 based on Western analysis shown in A were quantified and normalized to GAPDH; $n = 5-8$ for each group. (C) Absolute values for the clearance profile of STA-2842 represented by plasma concentration and kidney concentration (see Fig. 4H for kidney:plasma ratio). $n = 3$ WT mice; $n = 5-6$ *Pkd1*^{-/-} mice; * $P \leq 0.05$, *** $P \leq 0.005$; n/s, not significant. (D) Western blot analysis of kidney lysates of 5-mo-old *Pkd1*^{-/-} or control mice 12 h and 48 h after a single dose of STA-2842 (75 mg/kg), analyzed with indicated antibodies. Lysates from control mice are loaded as internal reference on both membranes. Left and right panels represent two membranes processed in parallel for each experiment. $n = 3$ for each WT group, and $n = 6-7$ for each *Pkd1*^{-/-} group. (E) Association analysis between cyst volume and the expression level of the indicated proteins determined by Western blot analysis as described in Fig. 5H. Dots represent individual mice of the indicated treatment groups. P values from left to right: 0.006; <0.001; <0.001; <0.001.

Dataset S1. Reverse phase protein array (RPPA) analysis

[Dataset S1 \(XLS\)](#)

Complete dataset for RPPA analysis, describing changes in expression of 160 proteins or phosphoproteins of *Pkd1*^{-/-} primary kidney cells 24 h after treatment with 250 nM STA-2842 or vehicle and complete dataset for RPPA analysis, showing changes in expression of 136 proteins or phosphoproteins analyzed by RPPAs in primary kidney lysates derived from *Pkd1*^{-/-} and WT mice, treated with a single dose of 75 mg/kg STA-2842 or vehicle for 12 h, as indicated.